I&EC research
Industrial & Engineering Chemistry Research

Article

pubs.acs.org/IECR

Exponential Function Shortcut Method for the Calculation of the Number of Theoretical Plates in a Distillation Column

Rui Cao,[†,‡,∥] Guolei Fu,[§] Huaming Guo,*[,†] Yansheng Liu,*[,‡] Yixuan Tang,[‡] Yan Wu,[‡] and Xianjian Zhang[§]

[†]School of Water Resources and Environment, China University of Geosciences (Beijing), Beijing 100083, PR China

[‡]State Key Laboratory of Heavy Oil Processing, China University of Petroleum, Beijing 102249, PR China

[§]China Tianchen Engineering Corporation, Tianjin 300400, PR China

ABSTRACT: An exponential function shortcut calculation (EFSC) method is proposed for the estimation of the number of theoretical plates, N_T, in distillation units. We set up the new concept of the thermal state equation, β-line equation, and define the cut ratio of the q line, δ, as an independent variable to interpret the stage separating capacity. The EFSC model is established on the basic data of N_T calculated by the previously presented exponential function rigorous calculation (EFRC) method. The data sources of the EFSC method are much greater than those of the Gilliland correlation. The curves of the EFSC model go through the points $(X = 0, Y = 1)$ and $(X = 1, Y = 0)$, whose physical significance fully coincides with the characteristics of $R \sim N_T$. Validation of the EFSC method indicates that its accuracy is close to that of the plate-to-plate calculations and the EFRC method and higher than that of the Gilliland correlation.

1. INTRODUCTION

Distillation has been the widely used separation technique in bulk refinery and chemical industries. It is unlikely that distillation will be replaced by alternative separation processes.[1] Shortcut methods are commonly used for calculating the number of theoretical plates in a distillation column, in addition to rigorous approaches, such as plate-to-plate calculations and graphical[2] and analytical methods.[3] They are applicable when estimating the number of theoretical plates and determining the optimum reflux ratio,[4] especially to serve as good initial guesses in the rigorous calculation of process simulation. Shortcut procedures provide an easy way of understanding the global behaviors of complex systems. It is not necessary for a shortcut model to solve systems of stiff differential equations. Accordingly, shortcut methods are more convenient and robust than rigorous methods, thus allowing the evaluation of alternatives without the requirement of a full specification.[5] Although computers have made it possible to solve large-scale models in a reasonable amount of time, shortcut models are necessary to derive global properties, such as feasible regions of operation, which are critical for iteration design, optimization, optimal control, and synthesis problems.[6] Therefore, shortcut methods are the best method for screening the scheme from a large number of alternatives in a short time.

The Fenske−Underwood−Gilliland method[7−9] (Gilliland method for short) is the most common shortcut approach, which has been widely used by the typical commercial process simulation software, such as Aspen plus and Pro/II, etc. In this method, Gilliland[9] made a great contribution to characterizing the relationship between the number of theoretical plates, N_T, and the reflux ratio, R. He investigated 61 industrial design data points in realistic evaluation and plotted the $X \sim Y$ diagram with $X = (R - R_{min})/(R + 1)$ and $Y = (N_T - N_{Tmin})/(N_T + 1)$, where $N_{T,min}$, the minimum number of theoretical plates at total reflux, was calculated by the Fenske equation[7] and R_{min}, the minimum reflux ratio, was determined by the Underwood equation.[8] Subsequently, Liddle,[10] Van Winkle and Todd,[11] Hohmann and Lockhart,[12] Molokanov et al.,[13] and Eduljee,[14] brought forward the correlations of $X \sim Y$ based on a Gilliland diagram. Those given by Molokanov et al.[13] and Eduljee[14] are the more popular equation forms. Additionally, Zuiderweg,[15] Salomone et al.,[16] and Lotter and Diwekar[17] used the Gilliland method for calculating batch distillations. Hengstebeck[18] and Liu et al.[19] developed the Gilliland method for separating the homogeneous azeotropic mixtures.

Moreover, Winn[20] proposed another method for the calculation of $N_{T,min}$. The vapor−liquid equilibrium constant, K, was introduced in the equilibrium equation instead of the relative volatility, α. In this method, a linear relation is shown between K and temperature at a fixed pressure. Thus, the parameters of this equation are constants for a given system, which would not vary with temperature. The Winn method seems more robust than the Fenske equation where α is dependent on temperature. Therefore, Aspen plus adopts the Winn method for calculating N_{Tmin} instead of the Fenske equation. In addition, Levy et al.[21] and Bausa et al.[22] proposed the boundary value method and the rectification body method, respectively, for determining R_{min}. The two approaches have both improved the Underwood models[4] by combining with the detailed heat-integration models, where a triangular diagram is used to represent the compositions. Therefore, they can be used for visualization of nonideal multicomponent systems.

The finite element difference approach[23] was also applied for the plate-to-plate calculations. It transformed a nonlinear difference equation into a linear one with the introduction of

Received: April 18, 2014
Revised: August 3, 2014
Accepted: August 29, 2014
Published: August 29, 2014

ACS Publications © 2014 American Chemical Society

dx.doi.org/10.1021/ie501603n | *Ind. Eng. Chem. Res.* 2014, 53, 14830−14840

a model parameter which was given by the combination of the operating-line equation and the equilibrium equation. Then, N_T was calculated with the liquid composition of final stage, x_n. Furthermore, Gentry[24] proposed a method of quasilinearization for numerical solution of a stepwise distillation process. Bachadori and Vuthaluru[25] established an empirical equation describing the relation between N_{Tmin}/N_T and L/V, where L/V is the ratio of the liquid flow rate (kilomoles per hour) to the vapor flow rate (kilomoles per hour).

Guerreri[26] compared the Gilliland,[9] finite element difference,[23] Winn,[20] and plate-to-plate calculations methods. He believed that the optimum results were obtained with the Gilliland method merely at $x_F = 0.5$ and $q = 1.0$, where x_F is the feed composition (mole percent) and q is the feed-thermal-state parameter. Similarly, the Winn method gives the best accuracy for $q = 1$ and $q = 0$, yet less approximate results for the flashed, subcooled, or superheated feed. The effects of q on R_{min} were not considered in the finite difference method, and there might be no definite results in some instances.

In addition, the approximate solutions of the rigorous method, such as Lewis[27] and Smoker[28] methods, have been presented as a shortcut calculation. The Lewis[27] and Smoker[28] methods are algebraic methods in which N_T can be obtained directly without stepwise calculation. Nevertheless, it is difficult to get their rigorous solutions. Said[29] gave the simplified solution of the Lewis equation, and Strangio and Treybal,[30] Jafarey et al.,[31] Douglas and Jafarey,[32] and Tolliver and Waggoner[33] presented the approximate solutions of the Smoker equation. Their accuracy, however, decreased after simplification, which was declared in our previous study.[34]

In general, the Gilliland method is the most popular one, which has been established on the industrially simulated data. The long-term commercial applications have lasted for over 70 years. However, this approach has some drawbacks of the constraints of the industrial maturity and computation level available at that time. There are only 61 data points in the Gilliland diagram with centralized distribution, which reduces the accuracy of the correlations, especially for the operations close to the minimum or total reflux. The curves of the above-mentioned correlations[10−14] do not fully coincide with the characteristics of $R \sim N_T$ because they do not go through the points $(X = 0, Y = 1)$ and $(X = 1, Y = 0)$. However, due to the lack of a simple analytical algorithm for solving the nonlinear equations, the calculation of N_T mainly depends hitherto on the plate-to-plate calculations. Because it is extremely difficult to expand the basic data for the establishment of shortcut models, the Gilliland method[9] is still in use today.

In our previous study, we brought forward the exponential function rigorous calculation (EFRC) method for the calculation of N_T.[34] In the multistage calculations, the relation between the liquid compositions of two arbitrary theoretical plates is nonlinear. By using the EFRC method we can transform the complex nonlinear function into the exponential function. Thus, the fractional number of stages can be obtained conveniently without plate-to-plate calculations. As an algebraic approach, the EFRC method[34] can optionally set the operating conditions and physical properties and therefore permits us to establish the new basic data in a wide scope, with 2323 data points. These data points cover almost all the ordinary application scopes in industry and are much more comprehensive than those of the Gilliland method.

Furthermore, in this work, we define the new concepts of condensation fraction on a theoretical plate, β, and its thermal-state equation, β-line equation, in accordance with the principle of multistage distillation. The work reveals the essence of the reflux ratio, R, in mass-transfer processes from the new view of thermal driving force. Consequently, a new independent variable, δ, the cut ratio of the q line, is introduced which contains more affecting factors than R. On the basis of δ and the new database, we have developed a novel shortcut model for calculating the number of theoretical plates.

The objectives of this study are to (1) evaluate a new independent variable that can represent global properties around the entire column, according to the thermal principles of distillation; (2) obtain the basic data for N_T by using the exponential function rigorous calculation (EFRC) method;[34] and (3) develop an exponential function shortcut calculation (EFSC) model by fitting these essential data.

2. EXPONENTIAL FUNCTION SHORTCUT CALCULATION METHOD

2.1. Thermal State Equation of Stage and New Independent Variable. *2.1.1. Condensation Fraction and Thermal State Equation of Stage.* Homogeneous mixtures can be separated through distillation process with external energy. Reflux liquid (or boilup vapor) is considered to be the cooling (or heat) source in distillation process, thus providing the mass-transfer driving force for vapor and liquid phases. The cooling energy of reflux is the sum amount of the heat removed from each stage, which determines the separation ability of an operating system. Therefore, the reflux rate can be used to determine the fractional stage number for a given separation.

To specify the heat quantity taken away by reflux from each stage, the condensation fraction (viz. liquid fraction) on the stage is defined in eq 1:

$$\beta = \frac{L}{M} \tag{1}$$

where β is the condensation fraction on stage, $\beta \in [0,1]$; M is the total streamflow rate on stage (kmol/h), and $M = V + L$; L and V are the liquid flow rate and the vapor flow rate on stage (kmol/h), respectively.

Assuming the constant molar overflow, for any theoretical stage the mass balance equation can be written as eq 2:

$$(1 - \beta)y_{i+1} + \beta x_{i-1} = z_{M,i} \tag{2}$$

where y_{i+1} and x_{i-1} are the composition of the vapor leaving the $i + 1$ stage and that of the liquid leaving the $i - 1$ stage (mol %), respectively; the stage number is counted from the top of the tower downward; $z_{M,i}$ is the hypothetical composition of total stream on the ith stage (mol %). Then, eq 2 is rewritten as eq 3:

$$y_{i+1} = \frac{\beta}{\beta - 1}x_{i-1} - \frac{1}{\beta - 1}z_{M,i} \tag{3}$$

Equation 3 is defined as the β-line equation, denoting the thermal states of vapor and liquid phases on any theoretical stage.

2.1.2. β-Line Equation on Single Stage and Multistage. Figure 1 illustrates the β-line of any single stage in a distillation column, which is presented as line AB in $y-x$ equilibrium diagram. The parameter β is expressed as β_R in the rectifying section and as β_S in the stripping section. It is worth noting that the vapor stream leaving the $i + 1$ stage of composition y_{i+1} and the liquid stream leaving the $i - 1$ stage of composition x_{i-1} are

dx.doi.org/10.1021/ie501603n | Ind. Eng. Chem. Res. 2014, 53, 14830−14840

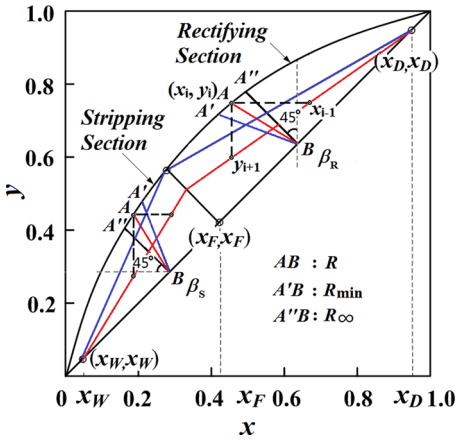

Figure 1. β-line in $y-x$ equilibrium diagram (single stage).

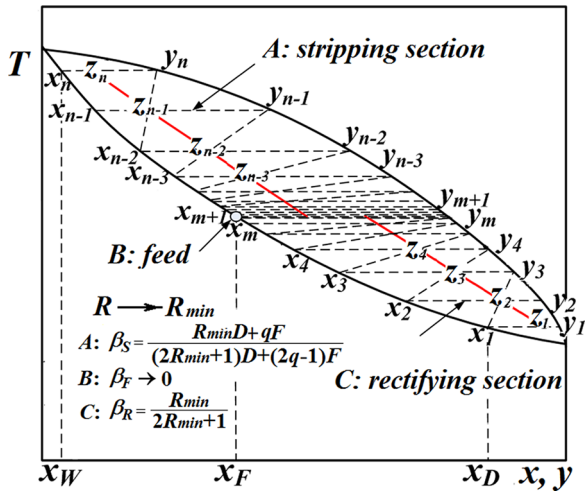

Figure 2. Value of β in $T-x-y$ equilibrium diagram at the minimum reflux (multistage).

mixed together at stage i and attain phase equilibrium after sufficient mass transfer, with the compositions y_i and x_i (mole percent), respectively. The β-line equation can be established based on the four passing streams at any single stage. Its slope, $\beta/(\beta - 1)$, being $-L_R/V_R$ (or $-L_S/V_S$), has the same absolute value as that of the operating line ($y = [R/(R + 1)]x + x_D/(R + 1)$ in the rectifying section and $y = [L_S/(L_S - W)]x - Wx_W/(L_S - W)$ in the stripping section) with an opposite gradient. In a sense, the β-line is similar to the operating line, which denotes the effect of reflux on separation capacity, namely, the active role of cooling/heat energy in mass-transfer driving force.

Consequently, the characteristics of the β-line on the multistage can be deduced from those of the single stage. We analyze the two limiting cases ($R = R_{min}$ and ∞) and then extend them to the operation at finite reflux. The specific discussions are shown below.

(1). Minimum Reflux. The minimum liquid rate is equivalent to the minimum cooling energy, which is distributed from the top of the tower downward and sequentially taken away at each stage. At the feed stage, the minimum residual cooling energy remaining represents the cooling energy for condensing a drop of liquid. The feed stage is by then under the state of dew point.

In an ideal system, there is almost no mass transfer between vapor and liquid phases on the feed stage because the liquid there is too little, where the operating line and the equilibrium line intersect and generate a pinch point. It can be deduced that at the feed stage $\beta_F \rightarrow 0$, $\Delta y \rightarrow \Delta y_{min} \rightarrow 0$, and $N_T \rightarrow \infty$, where $\Delta y (= y^* - y)$ is the mass-transfer driving force and y^* is the equilibrium concentration of x. The β-line of any other stage in the rectifying section and the stripping section at R_{min} is drawn as line A′B in Figure 1. Similar results can be obtained for nonideal system, although the pinch point may be the tangency point of the operating line and the equilibrium line.

The β values of all stages in a tower can be easily denoted by the level-arm rule in the $T-x-y$ diagram (see Figure 2), that is $\beta = L/(L + V) = (y_i - z_i)/(y_i - x_i)$, where z_i is the hypothetical composition of the sum stream of the vapor and liquid stream on stage i (mole percent), $z_i = (Vy_{i+1} + Lx_{i-1})/(V + L) = (Vy_i + Lx_i)/(V + L)$. As shown in Figure 2, the stages are made from the top of the tower downward or from the bottom of the tower upward according to the compositions of vapor and liquid phases, (x, y). The fractional number of stages approaches infinity at the feed location. Thus, we get $\beta_R = R_{min}/(2R_{min} + 1)$ on any stage in the rectifying section and $\beta_S = (R_{min}D + qF)/[(2R_{min} + 1)D + (2q - 1)F]$ in the stripping section, except the feed stage.

(2). Total Reflux. The amount of total reflux represents the maximum cooling energy removed from the column. There is no feed or product, and the overhead vapor is totally condensed at total reflux. In this case, $L = V$, so $\beta = 1/2$ and $\beta/(\beta - 1) = -1$ on any stage, and the mass-transfer driving force $\Delta y \rightarrow \Delta y_{max}$, $N_T \rightarrow N_{Tmin}$. The β-line of a single stage at total reflux is drawn as line A″B in Figure 1. Furthermore, as shown in Figure 3, the value of β for a multistage distillation at total reflux is illustrated in the $T-x-y$ diagram, where z_i is the midpoint of y_i and x_i because $\beta = 1/2$.

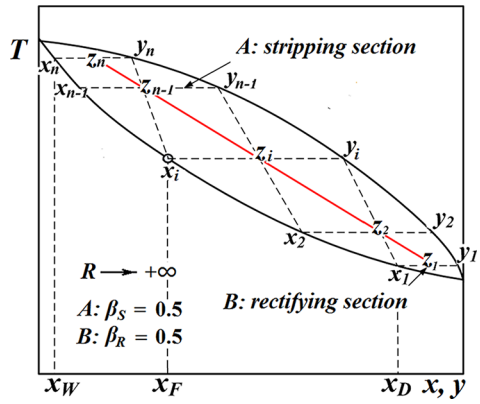

Figure 3. Value of β in $T-x-y$ equilibrium diagram at total reflux (multistage).

(3). Finite Reflux. At finite reflux, the feasible region of the β-line is confined between A′B and A″B (see Figure 1). That is, $\beta_R \in (0,1/2]$ and the β-line's gradient $\beta_R/(\beta_R - 1) = -(L_R/V_R) \in [-1,0)$ in the rectifying section, while $\beta_S \in [1/2,1)$ and $\beta_S/(\beta_S - 1) = -(L_S/V_S) \in (-\infty,-1]$ in the stripping section. With the limiting values of β given by Figures 2 and 3, we get the value scope of β for a multistage distillation and then characterize the β-lines in the $y-x$ diagram (as shown in Figure 4). All the β-lines in the rectifying section (or in the stripping section) are a group of parallel lines, which pass through the point (x_i, y_i), with the gradient of $-L_R/V_R$ (or $-L_S/V_S$). In other words, all the β-lines in a particular tower

dx.doi.org/10.1021/ie501603n | Ind. Eng. Chem. Res. 2014, 53, 14830−14840

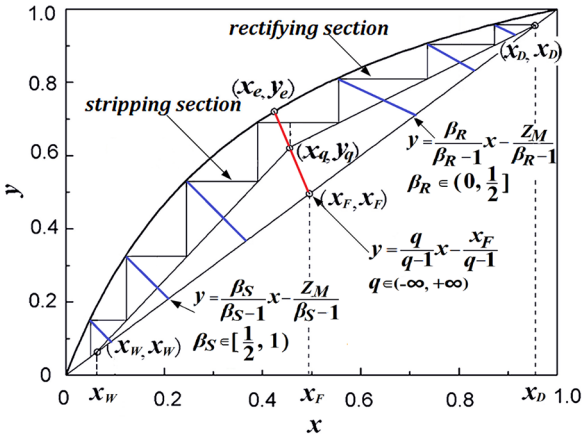

Figure 4. β-Line in $y-x$ equilibrium diagram ($0< q < 1$) (multistage).

section at fixed L and V are of similar graphical features and mathematical forms. Alternately, it denotes the correspondence between β and R so that we can determine N_T by using the β-line instead of the traditional operating line.

2.1.3. q-Line Equation: A Special β-Line Equation. The heat or cooling energy, as well as the thermodynamic data, determines the mass-transfer driving force. This is the direct basis for the calculation of N_T. Accordingly, in the former shortcut models of N_T, R was considered to be the independent variable. However, the fact might be ignored that the external heat or cooling energy of the feed can also alter the vapor or liquid load inside the column and result in the variation of separation capacity. In sum, the parameter R is not sufficient to reveal the comprehensive effects of the independent variables.

Therefore, both the thermal state of streams on each stage and that of the feed (q) should be taken into account in the selection of the new model's independent variable. The q line may be the best choice. The q-line equation is known as the feed-thermal-state equation, and the β-line equation is defined as the staged-thermal-state equation. They have similar physical significance and model expressions, which indicates that the q-line is a special β-line. Because the β-line gives the implication of R and the feed stage, joining the rectifying and stripping sections, is of great importance for the representation of whole column's characteristics, the independent variable can be found based on the q-line equation (eq 4).

$$y = \frac{q}{q-1}x - \frac{x_F}{q-1} \tag{4}$$

As shown in Figure 4, one end of the q-line meets the equilibrium line at the point (x_e, y_e), and the other end intersects the line of $y = x$ at the point (x_F, x_F), indicating the operating range from R_{min} to R_{max} at a given q, namely, the feasible range of heat removal from the minimum to the maximum amount at the corresponding feed thermal state. We defined it as the maximum operating margin of the reflux. Moreover, the cross point (x_q, y_q) of the two operating lines and the q-line gives the implications of R (actual heat removal) and q (heat provided by feed), simultaneously. The distances between the cross point (x_q, y_q) and the point (x_e, y_e) or between (x_q, y_q) and (x_F, x_F) stand for the margins from the actual reflux to the minimum or maximum reflux, respectively, that is, the ratio of the margins from the actual heat removal to the minimum or maximum one at given feed thermal state. The relation between the mass-transfer driving force and this ratio is certified in the following part of this paper. We hereby introduce a new independent variable: the cut ratio of the q-line.

2.1.4. Definition of the Cut Ratio of the q-Line. The cut ratio of the q-line, δ, is defined as the length ratio of the two segments of the q-line, which is divided by the point (x_q, y_q) (see eq 5). It is illustrated by the state of $0 < q < 1$ in Figure 5.

$$\delta = \frac{l_1}{l_2} = \frac{\sqrt{(y_e - y_q)^2 + (x_e - x_q)^2}}{\sqrt{(y_q - x_F)^2 + (x_q - x_F)^2}} \tag{5}$$

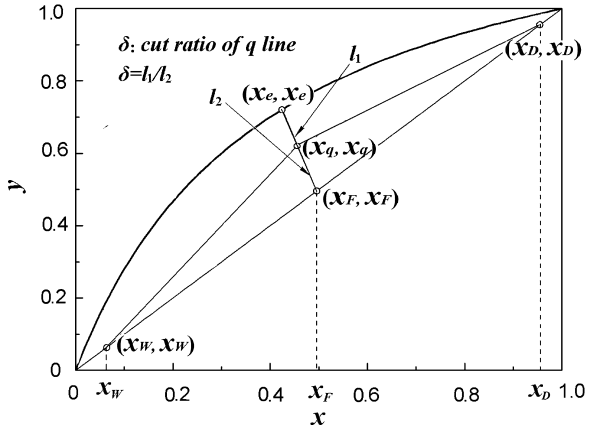

Figure 5. Definition of δ, the cut ratio of the q-line ($0 < q < 1$).

where l_1 is the length of the q-line segment from the point (x_e, y_e) to the point (x_q, y_q); l_2 is that from the point (x_q, y_q) to the point (x_F, x_F).

The independent and dependent variables of this model are normalized so as to conveniently show the limiting values at the minimum and total reflux, i.e., $X = (\delta - \delta_{min})/(\delta + 1)$ and $Y = (N_T - N_{Tmin})/(N_T + 1)$. Additionally, δ and N_T are required to meet the following objectives:

(1) All the values of X and Y are confined in [0,1].
(2) The functions of $\delta(X)$ and $N_T(Y)$ are monotonic.
(3) Y decreases with the increase of X, which coincides with the characteristic of $\delta \sim N_T$ curve.

Note that, at the minimum reflux, the point (x_q, y_q) overlaps the point (x_e, y_e), namely $\delta_{min} = 0$. Subsequently, $X = (\delta - \delta_{min})/(\delta + 1) = \delta/(\delta + 1)$, where the formulation of X is quite simple without the calculation of R_{min}.

On the basis of the definition of δ, the relation between $\delta/(\delta + 1)$ and β can be expressed as eq 6 (see Appendix I).

$$\frac{\delta}{\delta + 1} = \frac{l_1}{l_1 + l_2} = 1 - \frac{\sqrt{2q^2 - 2q + 1}\,(x_D - x_F)}{l_T\left(q - \frac{1}{2} - \frac{1}{4\beta_R - 2}\right)} \tag{6}$$

where l_T ($l_T = l_1 + l_2 = [(x_e - x_F)^2 + (y_e - x_F)^2]^{1/2}$) is related to only x_F, α, and q.

It can be found that (1) $\delta/(\delta + 1)$ is a monotonic function of β_R or β_S (see Appendix I), representing the effect of R; (2) $\delta/(\delta + 1)$ reflects the effect of q; and (3) $[\delta/(\delta + 1)]|_{Rmin} = 0$, $[\delta/(\delta + 1)]|_{R\infty} = 1$, and $[\delta/(\delta + 1)]|_{Rfinite} \in [0,1]$; Y decreases with the increase of X.

Thus, $\delta/(\delta + 1)$ meets the above requirements for the independent variable.

dx.doi.org/10.1021/ie501603n | Ind. Eng. Chem. Res. 2014, 53, 14830−14840

2.1.5. Significance of Normalized δ. $\delta/(\delta + 1) = l_1/l_T$, where l_1 indicates the actual operating margin of the reflux, denoting the gap between the actual heat removal quantity and the minimum one, and l_T is the distance between (x_F, y_F) and (x_e, y_e), namely the maximum available operating margin of the reflux, denoting the gap between the maximum heat removal quantity and the minimum one. Therefore, the physical meaning of $\delta/(\delta + 1)$ is $(R - R_{min})/(R_\infty - R_{min})$ for a given feed, i.e., the fraction of the margin of actual heat removal quantity in the margin of the maximum available heat removal quantity.

The relation between $\delta/(\delta + 1)$ and mass-transfer driving force,$(y_q^* - y_q)$, has been deduced in Appendix II, indicating that $\delta/(\delta + 1)$ increases with the increase of $(y_q^* - y_q)$. As mentioned, $\delta/(\delta + 1)$ increases with the increase of R shown in Appendix I. Accordingly, $(y_q^* - y_q)$ also increases with the increase of R. Therefore, $(y_q^* - y_q)$ has the monotonic relation with $\delta/(\delta + 1)$. In sum, $\delta/(\delta + 1)$ is the key for the determination of N_T, because N_T greatly depends on the mass-transfer driving force.

2.2. EFSC Model. *2.2.1. EFRC Method for the Calculation of N_T.* Previously, we have brought forward the exponential function rigorous calculation method for the calculation of N_T,[34] which has been mentioned in more detail in the literature. The principle of the EFRC method is shown in Figure 6.

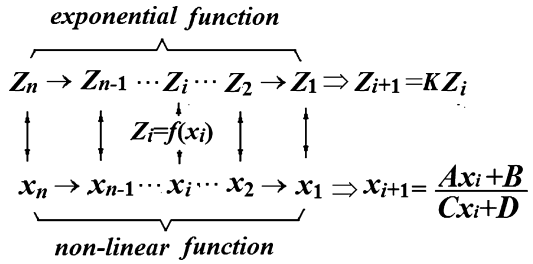

Figure 6. Principle of the EFRC method.

In terms of the equilibrium equation and the operating line equation, it has been found that the liquid compositions of any two adjacent stages satisfy the equation, $x_{i+1} = (Ax_i + B)/(Cx_i + D)$, where parameters A, B, C, and D are constants for a given process $(F, x_F, x_D, x_W, \alpha, R, q)$.[34] Because the correlation between x_{i+1} and x_i is nonlinear, it is difficult to get the algebraic solution of N_T. Therefore, we have constructed a monotonic function, $Z_i = (x_i + U)/(x_i + V)$, where parameters U and V are determined by parameters A, B, C, and D. In addition, Z_i is an exponential function, where $Z_{i+1} = KZ_i$ and $K = (A + UC)/(A + VC)$. As we know, an exponential function can be transformed into a linear function in logarithmic coordinates. In this way, $\{x_i\}$ can be replaced by $\{Z_i\}$, which helps us to get the analytic formula of Z_n. Herein, we present the rigorous algebraic solution of N_T (see eq 7).

$$N_R = \frac{\log(Z_m/Z_1)}{\log K} + 1, \quad N_S = \frac{\log(Z_n/Z_{m+1})}{\log K} \tag{7}$$

With the EFRC method, we can easily obtain the number of theoretical plates, feed location, and gas/liquid compositions of any theoretical plate without stepwise plate-to-plate calculations. In particular, it is much more convenient to get the value of $N_{T,min}$ for $Y = (N_T - N_{Tmin})/(N_T + 1)$ under total reflux because the EFRC method's parameters are $U = -1$, $V = 0$, and $K = \alpha$ (or $U = 0$, $V = -1$, and $K = 1/\alpha$) in that case.

2.2.2. Basic Data for the Establishment of the EFSC Model. There are 2323 basic data calculated by the EFRC method, considering most of the common operating conditions and physical properties of systems in industrial applications. These data are used to develop the EFSC model. The feasible application range is shown in Table 1, which indicates that a wider range of basic data has been obtained with the EFRC method,[34] in comparison with that of the Gilliland method.[9]

Table 1. Range of Basic Data for the Establishment of the EFSC Model

item	EFSC method	Gilliland method
R_{min}	0.49−44.56	0.53−9.09
R	0.50−560	
q	−0.5, 0, 0.5, 1, 1.5	0.28−1.42
a	1.05, 1.2, 1.5, 2.0, 2.5, 3.0, 3.5, 4.0, 4.5, 5.0	1.11−4.05
N_{Tmin}	4.56−151	3.4−60.3
N_T	4.59−728	

On the basis of the range of Table 1, the Y∼X curves are shown in Figures 7−9.

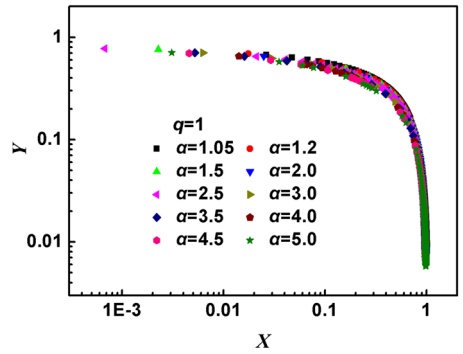

Figure 7. Y∼X curves of the EFSC method at different α (q = 1).

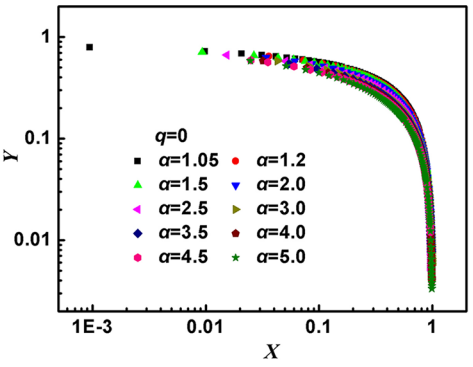

Figure 8. Y∼X curves of the EFSC method at different α (q = 0).

The Y∼X curves at the bubble point and the dew point under different α are plotted in Figures 7 and 8, respectively. The profiles of the Y∼X curves are analogous to the exponential function, namely, the radian of the curves increases monotonously with α. Therefore, the EFSC model is expressed as the exponential function. Additionally, the Y∼X curves at α = 2.5 with different q are shown in Figure 9, where the curves overlap each other. This result clearly indicates that the feed

dx.doi.org/10.1021/ie501603n | Ind. Eng. Chem. Res. 2014, 53, 14830−14840

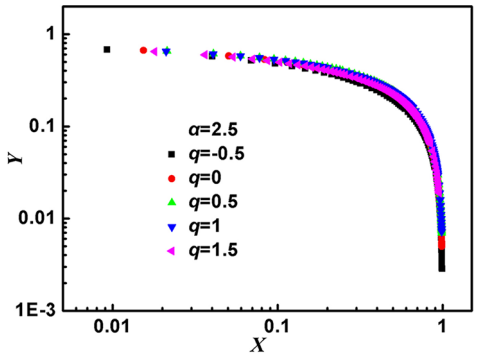

Figure 9. Y∼X curves of the EFSC method at different q (α = 2.5).

state has no significant effect on Y∼X curves because q has been included in the definition of δ. Thus, only α should be considered in the EFSC model, among the general adjustable parameters R, q, and α.

2.3. Construction and Error Analysis of the EFSC model. As mentioned above, the model is characterized as an exponential function with a single parameter, α. By the regression of the basic data, the EFSC model is established as eq 8.

$$Y = \alpha^{X(X-1)}(1 - X^{0.4318}) \tag{8}$$

The error analysis is shown in Figure 10. The average relative deviation of the new model, compared with the EFRC method,[34] is ±4.68%, with the maximum value of ±7.12%. The correlation coefficient of 0.9988. As shown in eq 8, the curves of the new model pass through the points (X = 0, Y = 1) and (X = 1, Y = 0), whose physical significance fully coincides with the characteristics of $R \sim N_T$.

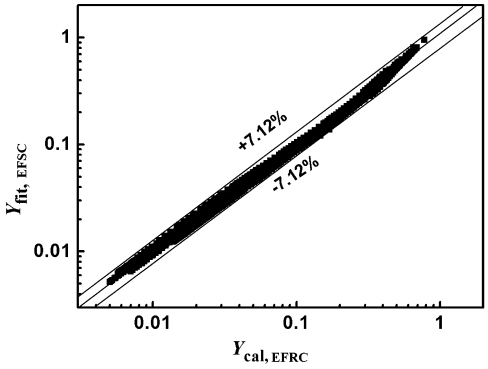

Figure 10. Error analysis of the EFSC model.

3. MODEL VALIDATION

Three cases have been used to validate the EFSC model by comparisons with the plate-to-plate calculations,[26] EFRC method,[34] and Gilliland correlation.[14] Case 1 and case 2 are the assessments for a multicomponent system and nonideal system, respectively. Thereafter, we give a wide scope of α in case 3 so as to evaluate the EFSC model's adaptability for various systems, where each value of α corresponds to a particular separating capacity.

Case 1: A continuous process for the separation of benzene + toluene + paraxylene system at atmospheric pressure was used for comparisons. We know that $x_{F,benzene}$ = 34.44% (mol %), $x_{F,toluene}$ = 48.67% (mol %), $x_{D,toluene}$ = 1.50% (mol %), and $x_{W,benzene}$ = 2.00% (mol %). The values of R and q are shown in Table 2. The four approaches have been used to calculate N_T.

In this study, the absolute difference in N_T between the evaluated method and the reference method's results is defined as

$$\Delta N_T = N_{T,\text{evaluated method}} - N_{T,\text{reference method}} \tag{9}$$

where $N_{T,evaluated\ method}$ is the result of the EFRC, Gilliland, or EFSC method ($N_{T,EFRC}$, $N_{T,Gilliland}$, or $N_{T,EFSC}$, respectively) and $N_{T,reference\ method}$ is that of the plate-to-plate calculations. The detailed results are shown in Table 2. It can be seen that the results of the EFSC method are close to those of the plate-to-plate calculations[24] and the EFRC method[34] and are better than those of the Gilliland correlation.[14]

Case 2: A continuous process for the separation of ethanol−water system at atmospheric pressure was used for comparisons. We know that $x_{F,ethanol}$ = 40.0% (mol %), $x_{D,ethanol}$ = 84.0% (mol %), and $x_{W,ethanol}$ = 4.0% (mol %) at more common industrial relevant reflux ratio, R/R_{min} = 1.5, and q = 1.3, 1, 0.5, 0, −0.2. The three approaches have been used to calculate N_T.

Because ethanol−water is highly nonideal with α varying from 1.161 to 11.71, we must handle it in a sectional way. In case 2, the operating composition range has been divided into eight sections. The average value of α_i in each section, Δx_i, was estimated based on the equilibrium data. Then, we obtained the sectional theoretical plate number, N_{Ti}, and sequentially obtained the total plate number, N_T, by adding all the values of N_{Ti} together. The results are shown in Table 3, and the

Table 2. Results of the EFSC Method, Plate-to-Plate Calculations, EFRC Method, and Gilliland Correlation (Benzene−Toluene−Paraxylene)

R/R_{min}	R_{min}	R	q	$N_{T,plate\text{-}to\text{-}plate}$	$N_{T,EFRC}$	ΔN_T[a]	$N_{T,Gilliland}$	ΔN_T[b]	$N_{T,EFSC}$	ΔN_T[c]
1.25	1.459	1.824	1.3	19.47	20.12	0.65	18.48	−0.99	19.69	0.22
	1.748	2.185	1	19.08	18.96	−0.12	17.94	−1.14	19.94	0.86
	2.510	3.138	0.5	18.63	18.16	−0.47	17.69	−0.94	19.20	0.57
	3.585	4.481	0	14.57	15.13	0.56	16.94	2.37	16.28	1.71
	6.160	7.700	−1	12.28	13.13	0.85	17.01	4.73	15.10	2.82
1.40	1.459	2.043	1.3	17.02	17.16	0.14	16.12	−0.90	17.35	0.33
	1.748	2.447	1	16.71	16.91	0.20	15.94	−0.77	16.34	−0.37
	2.510	3.514	0.5	15.97	15.95	−0.02	15.71	−0.26	15.79	−0.18
	3.585	5.019	0	13.25	13.47	0.22	14.97	1.72	13.65	0.40
	6.160	8.624	−1	11.53	11.98	0.45	15.03	3.50	13.07	1.54

[a] $\Delta N_T = N_{T,EFRC} - N_{T,plate\text{-}to\text{-}plate}$. [b] $\Delta N_T = N_{T,Gilliland} - N_{T,plate\text{-}to\text{-}plate}$. [c] $\Delta N_T = N_{T,EFSC} - N_{T,plate\text{-}to\text{-}plate}$.

dx.doi.org/10.1021/ie501603n | Ind. Eng. Chem. Res. 2014, 53, 14830−14840

Table 3. Results of the EFSC Method, Plate-to-Plate Calculations, and Gilliland Correlation (Ethanol−Water)

R/R_{min}	R_{min}	R	q	$N_{T,plate\text{-}to\text{-}plate}$	$N_{T,Gilliland}$	ΔN_T[a]	$N_{T,EFSC}$	ΔN_T[b]
1.5	1.67	2.51	1.3	18.32	20.87	2.55	19.77	1.45
	1.67	2.51	1	18.44	20.87	2.43	18.45	0.01
	1.67	2.51	0.5	18.78	20.87	2.09	17.08	−1.70
	1.67	2.51	0	19.16	20.87	1.71	17.75	−1.41
	1.72	2.59	−0.2	19.02	20.80	1.78	19.84	0.82

[a] $\Delta N_T = N_{T,Gilliland} - N_{T,plate\text{-}to\text{-}plate}$ [b] $\Delta N_T = N_{T,EFSC} - N_{T,plate\text{-}to\text{-}plate}$

Table 4. Illustration for the Calculation of N_T with the EFSC Method (Ethanol−Water)

$q = 1$	Δx_i	0.84−0.7	0.7−0.6	0.6−0.5	0.5−0.4	0.4−0.3	0.3−0.2	0.2−0.1	0.1−0.04	N_T
	α_i	1.179	1.416	1.714	2.148	2.852	3.898	5.804	11.705	
	$N_{i,EFSC}$	7.074	2.225	1.433	1.077	0.882	0.805	0.839	4.111	18.45

Table 5. Results of the EFSC Method, EFRC Method, and Gilliland Correlation at Different α and q ($R/R_{min} = 1.5$)

q	α	R	R_{min}	$N_{T,EFRC}$	$N_{T,Gilliland}$	ΔN_T[a]	$N_{T,EFSC}$	ΔN_T[b]
−0.5	2.5	5.36	3.57	11.23	13.67	2.44	11.59	0.36
0	1.2	18.07	12.05	64.15	63.54	−0.61	63.83	−0.32
	1.5	8.32	5.55	28.57	29.50	0.93	28.21	−0.36
	2	5.07	3.38	16.43	17.92	1.49	16.16	−0.27
	2.5	3.99	2.66	12.22	13.93	1.71	12.04	−0.18
	3	3.45	2.30	10.04	11.86	1.82	9.92	−0.12
	3.5	3.12	2.08	8.69	10.57	1.88	8.62	−0.07
	4	2.90	1.94	7.75	9.68	1.93	7.72	−0.03
	4.5	2.75	1.83	7.07	9.02	1.95	7.07	0.01
	5	2.63	1.76	6.54	8.51	1.97	6.57	0.03
0.5	2.5	2.86	1.91	13.43	14.31	0.88	12.83	−0.60
1	1.2	16.18	10.79	66.01	63.67	−2.34	65.47	−0.54
	1.5	6.43	4.29	30.54	29.82	−0.72	29.96	−0.58
	2	3.18	2.12	18.51	18.52	0.01	18.09	−0.42
	2.5	2.10	1.40	14.37	14.76	0.39	14.14	−0.23
	3	1.56	1.04	12.22	12.89	0.67	12.19	−0.03
	3.5	1.23	0.82	10.89	11.79	0.90	11.04	0.15
	4	1.01	0.68	9.97	11.06	1.09	10.31	0.34
	4.5	0.86	0.57	9.30	10.55	1.25	9.81	0.51
	5	0.74	0.50	8.77	10.18	1.41	9.46	0.69
1.5	2.5	1.65	1.10	14.70	15.18	0.48	15.82	1.12

[a] $\Delta N_T = N_{T,Gilliland} - N_{T,EFRC}$ [b] $\Delta N_T = N_{T,EFSC} - N_{T,EFRC}$

detailed calculation procedures of $N_{T,EFSC}$ for $q = 1$ are illustrated in Table 4.

From Table 3, it was found that the results of the EFSC method are close to those of the plate-to-plate calculations and are better than those of the Gilliland correlation.[14]

Case3: A continuous process at atmospheric pressure for the separation of a binary mixture of given α was used for comparisons. We know that $x_{F,light\ component} = 44.0\%$ (mol %), $x_{D,light\ component} = 97.4\%$ (mol %), and $x_{W,light\ component} = 2.35\%$ (mol %); $R/R_{min} = 1.5$; $\alpha = 1.05, 1.2, 1.5, 2, 2.5, 3, 3.5, 4, 4.5, 5.0$; and $q = 1.5, 1, 0.5, 0, -0.5$. The values of α and q are shown in Table 5. The three approaches have been used to calculate N_T.

Because the system designed in case 3 can be any binary system satisfying the given value of α, we can comprehensively evaluate the accuracy of the EFSC model for various systems with different volatility. Furthermore, as a rigorous method, the EFRC method agrees well with the plate-to-plate calculations (see Table 2) and has been validated in our previous study.[32] Thus, for the sake of convenience, the EFRC method serves as the reference method instead of the plate-to-plate calculations in case 3.

The comparisons between the EFSC method[34] and Gilliland correlation[14] are shown in Table 5. The comparison indicates that the results of the EFSC method are quite close to that of the EFRC method,[34] and its accuracy is much higher than that of the Gilliland correlation[14] at the common industrial relevant reflux.

4. CONCLUSIONS

The exponential function shortcut calculation (EFSC) method is developed and evaluated for calculating the number of theoretical stages in a distillation column. By analyzing the mass-transfer driving force, we put forward the new concept of the thermal-state equation, β-line equation, from the cooling energy (or heat energy) of the streams on any theoretical plate. The cut ratio of the q-line, δ, has been introduced as an independent variable of the new model, based on the special β-line equation, the q-line equation.

The EFSC model is established according to the basic data of N_T calculated by the previously reported EFRC method.

dx.doi.org/10.1021/ie501603n | Ind. Eng. Chem. Res. 2014, 53, 14830−14840

Because the operating conditions and physical properties in the EFRC method can be set optionally, the practical field of the new model is much wider than that of Gilliland approach. Furthermore, factors with much greater effect are taken into account in the new model, including R, q, and α. The EFSC model curves pass through the points ($X = 0$, $Y = 1$) and ($X = 1$, $Y = 0$), which fully coincides with the characteristics of $R \sim N_T$.

The new model has been assessed by the cited data of the plate-to-plate calculations, EFRC method, and Gilliland correlation. The assessment indicates that the results of the new model are close to those of the plate-to-plate calculations and the EFRC method. The average relative deviation of N_T from the EFRC method is ±4.68%, with the maximum value of ±7.12%. The correlation coefficient of 0.9988. The precision of the new model is much higher than that of the Gilliland correlation.

APPENDIX I

(1) $\delta/(\delta + 1) \sim \beta_R$:

As shown in eq 6

$$\frac{\delta}{\delta + 1} = \frac{l_1}{l_1 + l_2} = \frac{l_T - l_2}{l_T} \tag{A1}$$

where,

$$l_T = l_1 + l_2 = \sqrt{(x_e - x_F)^2 + (y_e - x_F)^2} \tag{A2}$$

and

$$l_2 = \sqrt{(x_q - x_F)^2 + (y_q - x_F)^2} \tag{A3}$$

The operating-line equation of the rectifying section is expressed as

$$y = \frac{R}{R + 1}x + \frac{x_D}{R + 1} \tag{A4}$$

The q-line equation is written as

$$y = \frac{q}{q - 1}x - \frac{x_F}{q - 1} \tag{A5}$$

The equilibrium equation is shown as

$$y = \frac{\alpha x}{1 + (\alpha - 1)x} \tag{A6}$$

Combination of eqs A4 and A5 gives

$$x_q = \frac{x_D q + x_F R + x_F - x_D}{q + R}$$
$$y_q = \frac{x_D q + x_F R}{q + R} \tag{A7}$$

$$\therefore x_q - x_F = \frac{x_D q + x_F R + x_F - x_D}{q + R} - x_F = \frac{(q - 1)(x_D - x_F)}{q + R}$$

$$y_q - x_F = \frac{x_D q + x_F R}{q + R} - x_F = \frac{x_D q + x_F R - x_F q - x_F R}{q + R} = \frac{q(x_D - x_F)}{q + R}$$

$$\therefore l_2 = \sqrt{(x_q - x_F)^2 + (y_q - x_F)^2} = \sqrt{2q^2 - 2q + 1}\,\frac{x_D - x_F}{q + R} \tag{A8}$$

Combination of eqs A5 and A6 gives the follow results:

(a.) Assuming $q \neq 1$ and $q \neq 0$, we obtain

$$x_e = \frac{(\alpha - 1)(x_F + q) - \alpha + \sqrt{[\alpha - (\alpha - 1)(x_F + q)]^2 + 4q(\alpha - 1)x_F}}{2q(\alpha - 1)}$$

$$y_e = \frac{(\alpha - 1)(q - x_F) - \alpha + \sqrt{[\alpha - (\alpha - 1)(x_F + q)]^2 + 4q(\alpha - 1)x_F}}{2(q - 1)(\alpha - 1)}$$

(b.) Assuming $q = 1$, we obtain

$$x_e = x_F, \quad y_e = \frac{\alpha x_F}{1 + (\alpha - 1)x_F}$$

(c.) Assuming $q = 0$, we obtain $y_e = x_F$,

$$y_e = x_F, \quad x_e = \frac{x_F}{\alpha - (\alpha - 1)x_F} \tag{A9}$$

Substitution of eq A9 into eq A2 yields l_T, which is related to only x_F, α, and q, yet has nothing to do with R.

Thus, because $R = -(\beta_R/2\beta_R - 1)$, eq A1 can be rewritten as

$$\frac{\delta}{\delta + 1} = \frac{l_T - \sqrt{2q^2 - 2q + 1}\,(x_D - x_F)/(q + R)}{l_T} = 1 - \frac{\sqrt{2q^2 - 2q + 1}\,(x_D - x_F)}{l_T\left(q - \frac{1}{2} - \frac{1}{4\beta_R - 2}\right)} \tag{A10}$$

We can deduce from eq A10 that $\delta/(\delta + 1)$ monotonously increases with β_R.

(2) $\delta/(\delta + 1) \sim \beta_S$:

$$\because \beta_R = \frac{R}{2R + 1}, \quad \beta_S = \frac{RD + qF}{(2R + 1)D + (2q - 1)F}$$

$$\therefore \beta_R = \frac{qF - 2qF\beta_S + F\beta_S - D\beta_S}{2qF - 4qF\beta_S + 2F\beta_S - D} \tag{A11}$$

$$(\beta_R)' = \frac{D^2 - DF}{(2qF - 4qF\beta_S + 2F\beta_S - D)^2} = -\frac{DW}{(2qF - 4qF\beta_S + 2F\beta_S - D)^2} < 0 \tag{A12}$$

We can deduce from eq A12 that β_R monotonously decreases with β_S. Consequently, $\delta/(\delta + 1)$ monotonously decreases with β_S.

APPENDIX II

The relation between $(y_q^* - y_q)$ and $\delta/(\delta + 1)$ is demonstrated as follows:

1. $(y_q^* - y_q) \sim R$:

dx.doi.org/10.1021/ie501603n | Ind. Eng. Chem. Res. 2014, 53, 14830−14840

Substitution of x_q into eq A6 yields

$$y_q^* = \frac{\alpha x_q}{1 + (\alpha - 1)x_q} \tag{A13}$$

Subsequently, the mass-transfer driving force is derived from eq A7 and eq A13:

$$(y_q^* - y_q) = \frac{\alpha(x_D q + x_F R + x_F - x_D)}{q + R + (\alpha - 1)(x_D q + x_F R + x_F - x_D)} - \frac{x_D q + x_F R}{q + R} \tag{A14}$$

The analysis of the relation between $(y_q^* - y_q)$ and R, based on the value scope of q, is specified below:

(1.) $0 \le q \le 1$, $(y_q^* - y_q) \sim R$:

Taking derivative of R with respect to eq A14, we obtain

$$(y_q^* - y_q)' = \frac{\alpha(1 - q)(x_D - x_F)}{[q + R + (\alpha - 1)(x_D q + x_F R + x_F - x_D)]^2} + \frac{q(x_D - x_F)}{(q + R)^2} \tag{A15}$$

Then, we can deduce from eq A15 that $(y_q^* - y_q)' > 0$ if $0 \le q \le 1$ and x_F, x_D, and α are given, thus indicating that $(y_q^* - y_q)$ monotonously increases with the increase of R.

(2) $q > 1$, $(y_q^* - y_q) \sim R$:

On the basis of eq A7, it follows that

$$R = \frac{x_D q + x_F - x_D - x_q q}{x_q - x_F}$$

$$q + R = \frac{x_D q + x_F - x_D - x_F q}{x_q - x_F} = \frac{(x_D - x_F)(q - 1)}{x_q - x_F}$$

$$y_q = x_q + \frac{x_D - x_F}{q + R} = x_q + \frac{x_q - x_F}{q - 1} = \frac{q x_q - x_F}{q - 1} \tag{A16}$$

So, the mass-transfer driving force can be rewritten as

$$(y_q^* - y_q) = \frac{\alpha x_q}{1 + (\alpha - 1)x_q} - \frac{q x_q - x_F}{q - 1} \tag{A17}$$

Taking derivative of x_q with respect to eq A17, we obtain

$$(y_q^* - y_q)' = \frac{\alpha}{[1 + (\alpha - 1)x_q]^2} - \frac{q}{q - 1} = \frac{(q - 1)\alpha - q[1 + (\alpha - 1)x_q]^2}{[1 + (\alpha - 1)x_q]^2(q - 1)} \tag{A18}$$

Let $Y = (q - 1)\alpha - q[1 + (\alpha - 1)x_q]^2$. After taking the derivative of x_q, we obtain

$$Y' = -2q(\alpha - 1)[1 + (\alpha - 1)x_q] \tag{A19}$$

Note that when $q > 1$, $Y' < 0$, that is, Y monotonously decreases with the increase of x_q. In addition, because the process conditions, $0 < x_F < x_q < 1$, always holds if $x_{q,\min} \to 0$, $Y_{\max} \to -\alpha < 0$. It helps to deduce that $y < 0$ and $(y_q^* - y_q)' < 0$, namely, $(y_q^* - y_q)$ monotonously decreases with the increase of x_q.

Furthermore, taking the derivative of R with respect to eq A7, we have

$$(x_q)' = \frac{(x_D - x_F)(1 - q)}{(q + R)^2} \tag{A20}$$

when $q > 1$, $(x_q)' < 0$. Thus, x_q monotonously decreases with the increase of R.

So, we find that when $q > 1$ and x_F, x_D, and α are given, $(y_q^* - y_q)$ monotonously increases with the increase of R.

(3) $q < 0$, $(y_q^* - y_q) \sim R$:

The relation between $(y_q^* - y_q)$ and R falls into three cases, where the demonstrating process is similar to that given above:

(1) If $x_F \le [1/(\alpha - 1)][((1 - 1/q)\alpha)^{1/2} - 1]$, $(y_q^* - y_q)$ monotonously increases with the increase of R;

(2) If $x_F > [1/(\alpha - 1)][((1 - 1/q)\alpha)^{1/2} - 1]$ and $0 < x_q < (1/(\alpha - 1))[((1-1/q)\alpha)^{1/2} - 1]$, $(y_q^* - y_q)$ monotonously increases with the increase of R;

(3) If $x_q > [1/(\alpha - 1)][((1 - 1/q)\alpha)^{1/2} - 1]$, $(y_q^* - y_q)$ monotonously decreases with the increase of R.

As we know, $x_F > [1/(\alpha - 1)][((1 - 1/q)\alpha)^{1/2} - 1]$ or $x_q > [1/(\alpha - 1)][((1 - 1/q)\alpha)^{1/2} - 1]$ can be satisfied only if $x_F > x_D$, so case (2) and case (3) do not exist in distillation. Therefore, it can be proven that $(y_q^* - y_q)$ monotonously increases with the increase of R.

2. Considering the preceding proof, $\delta/(\delta + 1)$ monotonously increases with the increase of R, we can draw the conclusion that $\delta/(\delta + 1)$ monotonously increases with the increase of $(y_q^* - y_q)$.

AUTHOR INFORMATION

Corresponding Authors

*H.G.: e-mail, hmguo@cugb.edu.cn; tel, 86 10 8973 3288; fax, 86 10 8973 4159.

*Y.L.: State Key laboratory of Heavy Oil Processing, China University of Petroleum, Beijing 102249, PR China

Present Address

‖R.C.: Currently an associate professor at Chemical Engineering College, China University of Petroleum, Beijing 102249, PR China. E-mail:ctray@cup.edu.cn.

Notes

The authors declare no competing financial interest.

ACKNOWLEDGMENTS

The authors thank the National Natural Science Foundation of China (21176248) and Science Foundation of China University of Petroleum, Beijing (2462012KYJJ0319 and qzdx-2011-01) for financial support.

NOMENCLATURE

A,B,C,D = parameter
D = flow rate of overhead product (kmol/h)
F = feed flow rate (kmol/h)
K = parameter
L_R = liquid flow rate in rectifying section (kmol/h)
L_S = liquid flow rate in stripping section (kmol/h)
l_1 = length of q-line from (x_e, x_e) to (x_q, y_q)
l_2 = length of q-line from (x_q, y_q) to (x_F, x_F)
l_T = length of q-line from (x_e, y_e) to (x_F, x_F)
M = total stream flow rate on stage (kmol/h), $M = V+L$
N_R = number of theoretical plates in rectifying section
N_S = number of theoretical plates in stripping section
N_T = total number of theoretical plates
$N_{T\min}$ = minimum number of theoretical plates

q = feed-thermal-state parameter
R = reflux ratio
R_{finite} = finite reflux ratio
R_{min} = minimum reflux ratio
R_{∞} = total reflux ratio
T = temperature (K)
U = parameter
V = parameter
V_R = vapor flow rate in rectifying section (kmol/h)
V_S = vapor flow rate in stripping section (kmol/h)
W = flow rate of bottom product (kmol/h)
$X = \delta/(\delta + 1)$
x_D = composition of overhead product (mol %)
x_e = liquid composition of intersection of q-line and equilibrium line (mol %)
x_F = feed composition (mol %)
x_i = liquid composition of arbitrary theoretical plate (mol %)
x_q = liquid composition of intersection of rectifying operating line and stripping operating line (mol %)
x_W = composition of bottom product (mol %)
$Y = (N_T - N_{Tmin})/(N_T + 1)$
y_e = vapor composition of intersection of q-line and equilibrium line (mol %)
y_i = vapor composition of arbitrary theoretical plate (mol %)
y_q = vapor composition of intersection of rectifying operating line and stripping operating line (mol %)
z_M = hypothetical composition of total stream on theoretical plate (mol %)

Greek Letters

α = relative volatility
β = condensation fraction on theoretical plate, $\beta \in [0,1]$
δ = cut ratio of q-line, $\delta = l_1/l_2$
δ_{min} = δ at the minimum reflux ratio, $\delta_{min} = 0$

Subscripts

D = overhead product
e = intersection of q-line and equilibrium line
F = feed
i = number of arbitrary theoretical plate
M = total stream on theoretical plate
max = maximum
min = minimum
n = number of theoretical plates
q = intersection of rectifying operating line and stripping operating line
R = rectifying section
S = stripping section
T = total column
W = bottom product

REFERENCES

(1) Kunesh, J. G.; Kister, H. Z.; Lockett, M. J.; Fair, J. R. Distillation: Still towering over other options. *Chem. Eng. Prog.* **1995**, *91* (10), 43−54.
(2) McCabe, W. L.; Thiele, E. W. Graphical Design of Fractionating Columns. *Ind. Eng. Chem.* **1925**, *17* (6), 605−611.
(3) Pradeep, B. D. *Distillation Dynamics and Control*; China Petrochemical Press: Beijing, China, 1985.
(4) Seader, J. D.; Henley, E. J. *Separation Process Principles*; John Wiley & Sons, Inc.: New York, 1998.
(5) Jurgen, B.; Wolfgang, M. Shortcut design methods for hybrid membrane/distillation processes for the separation of nonideal multicomponent Mixtures. *Ind. Eng. Chem. Res.* **2000**, *39* (6), 1658−1672.
(6) Stefan, P. L.; Urmila, M. D. Shortcut models and feasibility considerations for emerging batch distillation columns. *Ind. Eng. Chem. Res.* **1997**, *36* (3), 760−770.
(7) Fenske, M. R. Fractionation of Straight-Run Pennsylvania Gasoline. *Ind. Eng. Chem.* **1932**, *24* (5), 482−485.
(8) Underwood, A. J. V. Fractional distillation of multicomponent mixtures. *Chem. Eng. Prog.* **1948**, *44* (8), 603−614.
(9) Gilliland, E. R. Multicomponent rectification − estimation of the number of theoretical plates as a function of the reflux ratio. *Ind. Eng. Chem.* **1940**, *32* (9), 1220−1223.
(10) Liddle, C. J. Improved shortcut method for distillation calculations. *Chem. Eng.* **1968**, *75* (23), 137−142.
(11) Van Winkle, M.; Todd, W. G. Optimum fractionation design by simple graphical methods. *Chem. Eng.* **1971**, *78* (21), 136−148.
(12) Hohmann, E. C.; Lockhart, F. J. Remember the hyperbola. *Chem. Technol. (Washington, DC, U. S.)* **1972**, *2* (10), 614−619.
(13) Molokanov, Y. K.; Korablina, T. P.; Mazurina, N. I.; Nikiforov, G. A. An approximate method of calculating the basic parameters of a multicomponent fractionation. *Chem. Technol. Fuels Oils* **1971**, *7* (2), 129−133.
(14) Eduljee, H. E. Equations replace Gilliland plot. *Hydrocarbon Process. (1966-2001)* **1975**, *54* (9), 120−122.
(15) Zuiderweg, F. J. Rapid calculation of plate number and reflux ratio in batch distillation. *Chem. Eng. Sci.* **1951**, *1* (1), 8−17.
(16) Salomone, H. E.; Chiotti, O. J.; Iribarren, O. A. Short-cut design procedure for batch distillations. *Ind. Eng. Chem. Res.* **1997**, *36* (1), 130−136.
(17) Lotter, S. P.; Diwekar, U. M. Shortcut models and feasibility considerations for emerging batch distillation columns. *Ind. Eng. Chem. Res.* **1997**, *36* (3), 760−770.
(18) Hengstebeck, R. J. An improved shortcut for calculating difficult multicomponent distillations. *Chem. Eng.* **1969**, *77* (1), 115−118.
(19) Liu, G. L.; Jobson, M.; Smith, R.; Wahnschafft, O. M. Shortcut design method for columns separating azeotropic mixtures. *Ind. Eng. Chem. Res.* **2004**, *43* (14), 3908−3923.
(20) Winn, F. W. New relative volatility method for distillation calculations. *Petroleum Refiner* **1958**, *37* (5), 216−218.
(21) Levy, S. G.; Van Dongen, D. B.; Doherty, M. F. Design and synthesis of homogeneous azeotropic distillations. 2. Minimum reflux calculations for nonideal and azeotropic columns. *Ind. Eng. Chem. Fundam.* **1985**, *24* (4), 463−474.
(22) Bausa, J.; Watzdorf, R. v.; Marquardt, W. Shortcut methods for nonideal multicomponent distillation: 1. Simple columns. *AIChE J.* **1998**, *44* (10), 2181−2198.
(23) Mickley, H. S.; Sherwood, T. K.; Reed, C. E. *Applied Mathematics in Chemical Engineering*, 2nd ed.; McGraw-Hill Book Company, Inc.: New York, 1957.
(24) Gentry, J. W. An improved method for numerical solution of distillation processes. *Can. J. Chem. Eng.* **1970**, *48* (4), 451−455.
(25) Bahadori, A.; Vuthaluru, H. B. Simple equations to correlate theoretical stages and operating reflux in fractionators. *Energy* **2010**, *35* (3), 1439−1446.
(26) Guerreri, G. Short-cut distillation design: Beware! *Hydrocarbon Process.* **1969**, *48* (8), 137−142.
(27) Lewis, W. K. The efficiency and design of rectifying column for binary mixture. *J. Ind. Eng. Chem. (Washington, D. C.)* **1922**, *14* (6), 492−496.
(28) Smoker, E. H. Analytical determination of plates in fractionating columns. *Trans. Am. Inst. Chem. Eng.* **1938**, *34* (12), 165−172.
(29) Said, A. S. A simple analytic formula for the number of theoretical plates in distillation. *Sep. Sci. Technol.* **1980**, *15* (10), 1699−1708.
(30) Strangio, V. A.; Treybal, R. E. Reflux-Stages Relations for Distillation. *Ind. Eng. Chem. Process Des. Dev.* **1974**, *13* (3), 279−285.
(31) Jafarey, A.; Douglas, J. M.; McAvoy, T. J. Short-cut techniques for distillation column design and control. 1. Column design. *Ind. Eng. Chem. Process Des. Dev.* **1979**, *18* (2), 197−202.

(32) Douglas, J. M.; Jafarey, A.; Seemann, R. Short-cut techniques for distillation column design and control. 2. Column operation and control. *Ind. Eng. Chem. Process Des. Dev.* **1979**, *18* (2), 203−210.
(33) Tolliver, T. L.; Waggoner, R. C. Approximate solutions for distillation rating and operating problems using the smoker equations. *Ind. Eng. Chem. Fundam.* **1982**, *21* (4), 422−427.
(34) Cao, R.; Fu, G. L.; Liu, Y. S.; Yan, C. Y.; Wu, Y.; Wang, J. Exponential function rigorous method for calculation of the number of theoretical plates in distillation column. *Chem. Eng. Sci.* **2012**, *84* (24), 628−637.